Neural interactions underlying visuomotor associations in the human brain

Radhika Madhavan*[1], Arjun K. Bansal*[1,6], Joseph R. Madsen[1], Alexandra J. Golby[3], Travis S. Tierney[3], Emad N. Eskandar[4], William S. Anderson[2] and Gabriel Kreiman[1,5]

[1]Departments of Ophthalmology and Neurosurgery, Children's Hospital, Harvard Medical School

[2]Department of Neurosurgery, Johns Hopkins Medical School

[3]Department of Neurosurgery, Brigham and Women's Hospital, Harvard Medical School

[4]Department of Neurosurgery, Massachusetts General Hospital

[5]Center for Brain Science, Harvard University

[6]Current affiliation: Nervana Systems, Inc.

* Both authors contributed equally

To whom correspondence should be addressed: gabriel.kreiman@tch.harvard.edu

Supplementary Figures: 12 figures

Supplementary Tables: 3 tables

Neural interactions underlying visuomotor associations in the human brain

Radhika Madhavan*[1], Arjun K. Bansal*[1,6], Joseph R. Madsen[1], Alexandra J. Golby[3], Travis S. Tierney[3], Emad N. Eskandar[4], William S. Anderson[2] and Gabriel Kreiman[1,5]

Supplementary Tables

Table S1: Distribution of electrode locations

Region name	# of electrodes	Average Talairach coordinates
G_temp_sup-Lateral	96	-44.5 -17.4 -2.8
G_temporal_middle	92	-38.6 -26.3 -7.9
G_front_middle	66	-9.3 27.4 19.1
G_temporal_inf	55	-20.4 -28.2 -21.2
G_pariet_inf-Supramar	53	-31.2 -31.3 32.9
G_precuneus	47	0.1 -53.7 40.1
Pole_temporal	46	-19.1 -1.4 -20.2
G_front_sup	43	6.9 22.3 46.0
G_orbital	43	-6.6 11.0 -14.0
G_oc-temp_med-Lingual	42	0.1 -62.8 5.6
G_pariet_inf-Angular	38	28.4 -56.2 50.1
G_precentral	38	-31.4 -1.9 38.3
G_oc-temp_med-Parahip	37	-5.9 -4.0 -18.2
G_cuneus	34	0.3 -78.4 27.4
G_postcentral	34	-21.7 -19.4 57.1
G_oc-temp_lat-fusifor	33	-6.7 -42.6 -14.2
G_front_inf-Opercular	28	-37.5 9.2 2.0
G_and_S_subcentral	25	-27.3 -12.5 10.7
G_front_inf-Triangul	21	-41.9 13.0 -7.7
Pole_occipital	21	12.0 -96.0 6.4
G_occipital_middle	17	8.6 -80.9 16.5
G_parietal_sup	11	18.3 -44.4 78.3
G_and_S_frontomargin	9	-11.8 44.7 -16.3
G_and_S_occipital_inf	9	37.7 -69.5 -10.0
S_intrapariet_and_P_trans	9	31.4 -62.1 72.8
G_and_S_transv_frontopol	8	2.7 42.2 -4.8
G_occipital_sup	8	16.1 -84.9 43.7
G_cingul-Post-dorsal	7	-0.8 -42.0 24.4
S_front_inf	7	-21.4 33.6 17.7
S_front_middle	7	8.4 33.6 11.8
S_orbital-H_Shape	7	3.7 21.8 -18.5
G_and_S_paracentral	6	9.3 -26.2 84.1
S_front_sup	6	31.0 23.7 49.9

S_temporal_sup	6	22.9 -49.3 18.2
G_rectus	5	10.7 -17.0 -17.2
G_temp_sup-Plan_tempo	5	-35.0 -28.4 15.7
S_central	4	36.5 -5.9 85.1
G_and_S_cingul-Mid-Ant	3	2.0 16.2 30.9
G_front_inf-Orbital	3	-38.2 -15.6 -23.3
G_temp_sup-Plan_polar	3	24.0 -13.8 -16.7
S_oc_sup_and_transversal	3	31.4 -79.7 52.0
S_pericallosal	3	1.8 21.6 20.2
S_subparietal	3	-0.8 -38.4 36.7
G_and_S_cingul-Ant	2	0.9 47.1 12.3
S_collat_transv_ant	2	-27.9 -33.0 -25.7
S_oc-temp_lat	2	-1.9 -49.3 -17.1
S_orbital_med-olfact	2	27.0 15.5 1.6
S_postcentral	2	-9.7 -45.5 58.1
S_precentral-sup-part	2	40.6 -12.6 57.9
G_subcallosal	1	1.3 11.3 -8.8
S_oc-temp_med_and_Lingual	1	17.6 -59.2 -7.8
S_orbital_lateral	1	49.5 46.2 -2.1
S_precentral-inf-part	1	-50.6 24.1 38.0
S_suborbital	1	2.6 62.2 -2.9
S_temporal_inf	1	-53.0 -8.0 -23.7
Total mapped	**1059**	
Unmapped (including depth electrodes)	**181**	
Total	**1240**	

This table reports the number of electrodes in each anatomical region. Region names are based on the parcellation in Destrieux *et al* (Destrieux et al., 2010). Average Tailarach coordinates are provided here for coarse orientation purposes only, it is not clear whether averaging in Tailarach space constitutes a meaningful operation.

Table S2: Number of visually responsive, motor-responsive and mapping-selective electrodes in different frequency bands. "Broadband" refers to the results reported in the main text based on the raw data from 0.1 to 500 Hz.

Frequency range (Hz)	Visually-responsive	Motor-responsive	Mapping selective
Broadband	87	67	35
4-8	61	75	13
8-12	41	27	13
12-35	94	60	2
35-50	93	15	1
70-100	135	23	4

Table S3: Distribution of mapping, visual and motor electrodes in each subject

Subject #	# Map. select.	# Vis. respon.	Poss. Map-Vis pairs	Map-Vis. pairs Fig. 6-7	# Motor respon.	Poss. Map-Motor pairs	Map.-Motor pairs Fig. 6-7	Poss. Vis-Motor pairs	Vis.-Motor pairs Fig. 6-7
1	0	4	0	0	6	0	0	24	0
2	0	3	0	0	12	0	0	36	0
3	0	7	0	0	0	0	0	0	0
4	4	2	8	6	0	0	0	0	0
5	2	0	0	0	1	2	0	0	0
6	15	51	765	552	1	15	7	51	51
7	0	3	0	0	23	0	0	69	0
8	0	8	0	0	3	0	0	24	0
9	10	1	10	10	3	30	27	3	3
10	3	2	6	6	0	0	0	0	0
11	1	4	4	4	0	0	0	0	0
12	0	2	0	0	18	0	0	36	0
Total	**35**	**87**	**793**	**578**	**67**	**47**	**34**	**243**	**54**

Number of electrodes that showed mapping selectivity, visual responsiveness and motor responsiveness in each subject (see **Methods** for definitions). The table also reports the number of *possible* pairs between these 3 groups (e.g. possible mapping-visual pairs = # mapping electrodes x # visual electrodes). Not all possible pairs were used for the coherence calculations: pairs with adjacent electrodes were excluded, pairs with electrodes in the same anatomical region were excluded, and only pairs in subjects that had mapping selective electrodes were included. The table reports the final number of electrode pairs that were used in **Figs. 6-7**.

Figure S1A

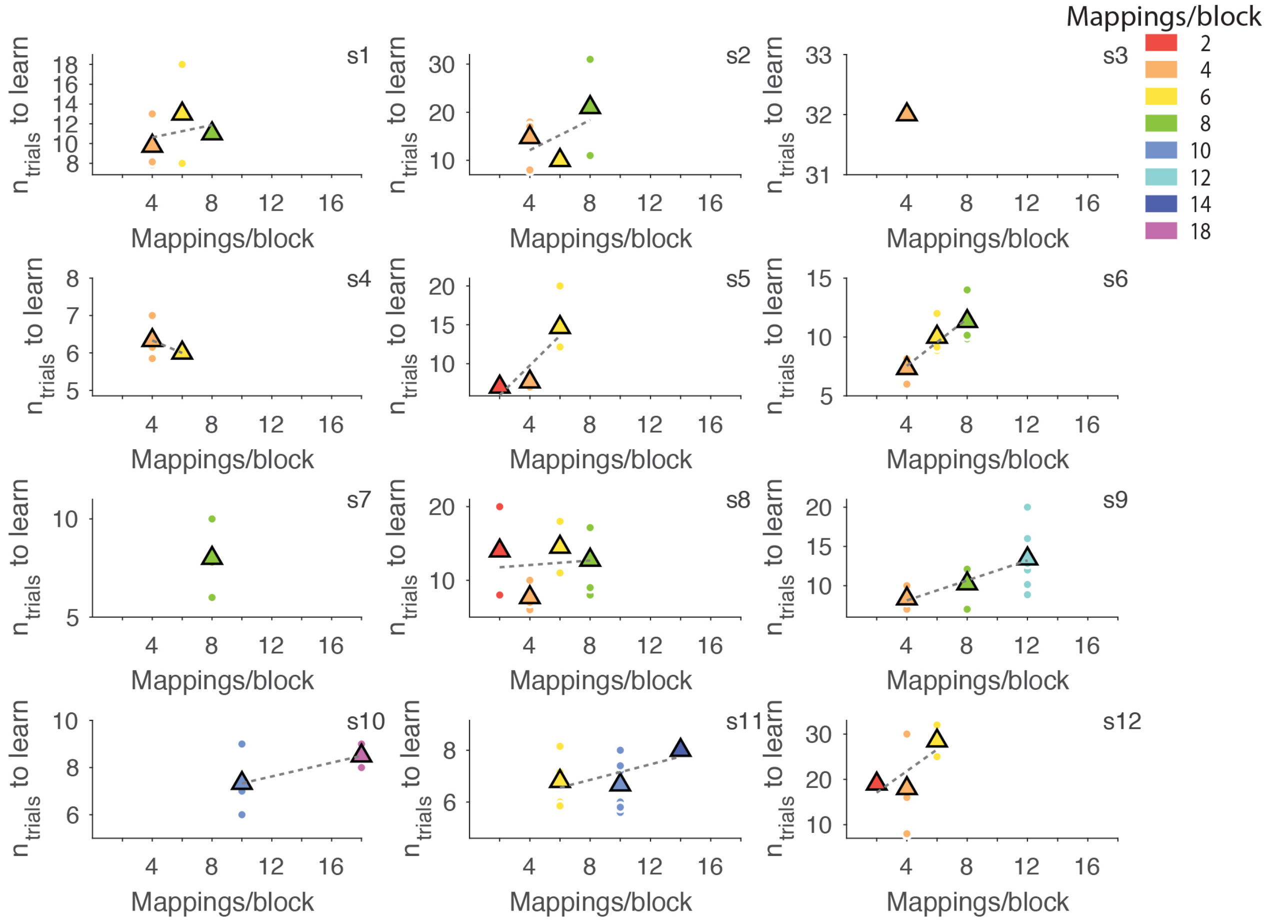

Figure S1A: More trials were required to reach learning criterion with increased number of mappings per block. Expanding on **Figure 1** in the main text, this figure shows the number of trials required to reach learning criterion (y-axis, **Methods**) for each mapping as a function of the number of mappings per block (x-axis) for each subject (s1-s12). Each dot denotes a single mapping, the color corresponds to the x-axis and is the same color used in **Figure 1B**. When two mappings required the exact same number of trials, the points are displayed along the y-axis for clarity. The triangles represent the average of all the learnt mappings for each block. The dotted line shows a linear regression fit (only when there is more than one block). Subjects 1-3 are different in that new mappings were added onto the old ones (**Methods**).

Figure S1B

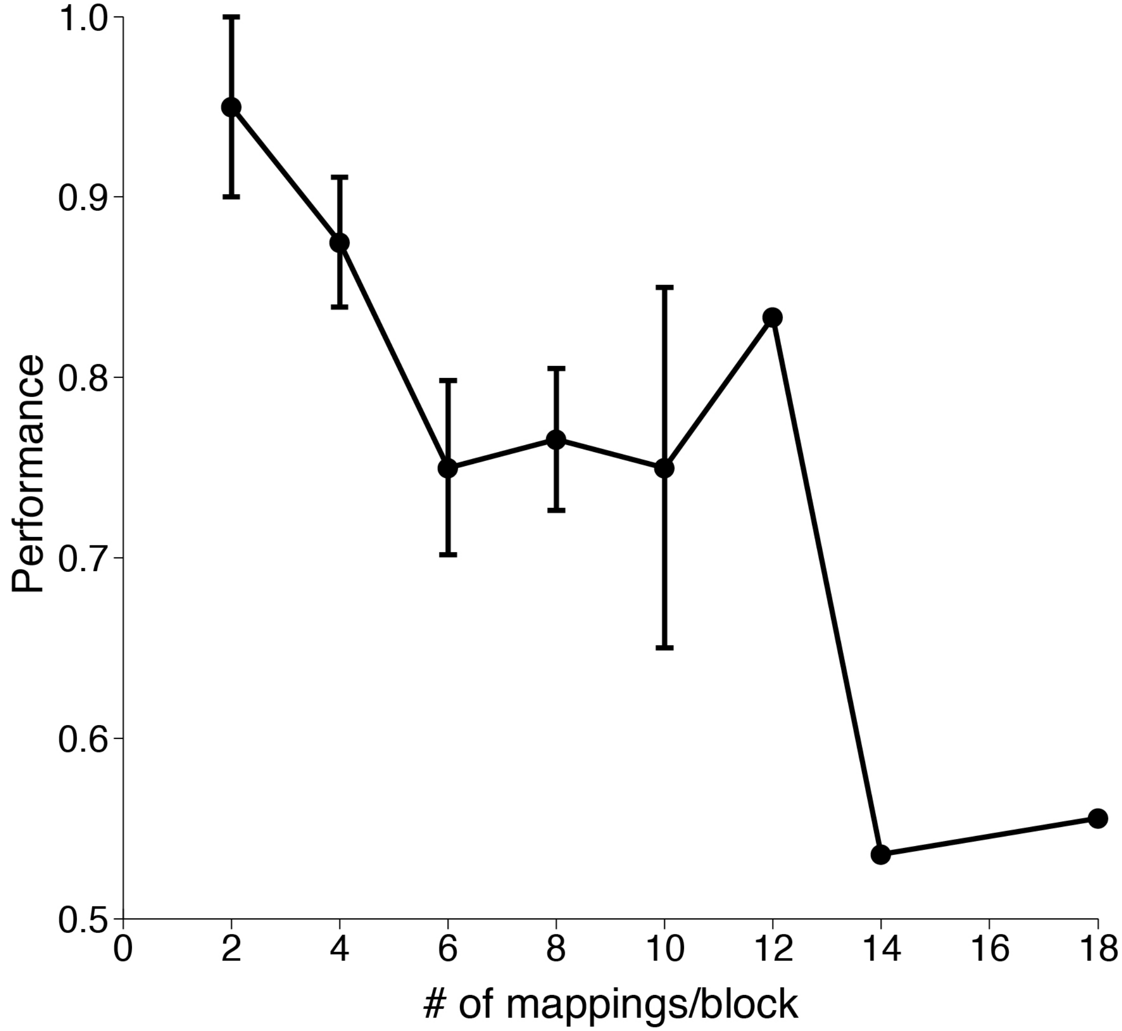

Figure S1B: Performance decreased with the number of mappings per block. Expanding on **Figure 1** in the main text, this figure shows the decrease in performance (averaged across subjects) as a function of the number of mappings per block.

Figure S2

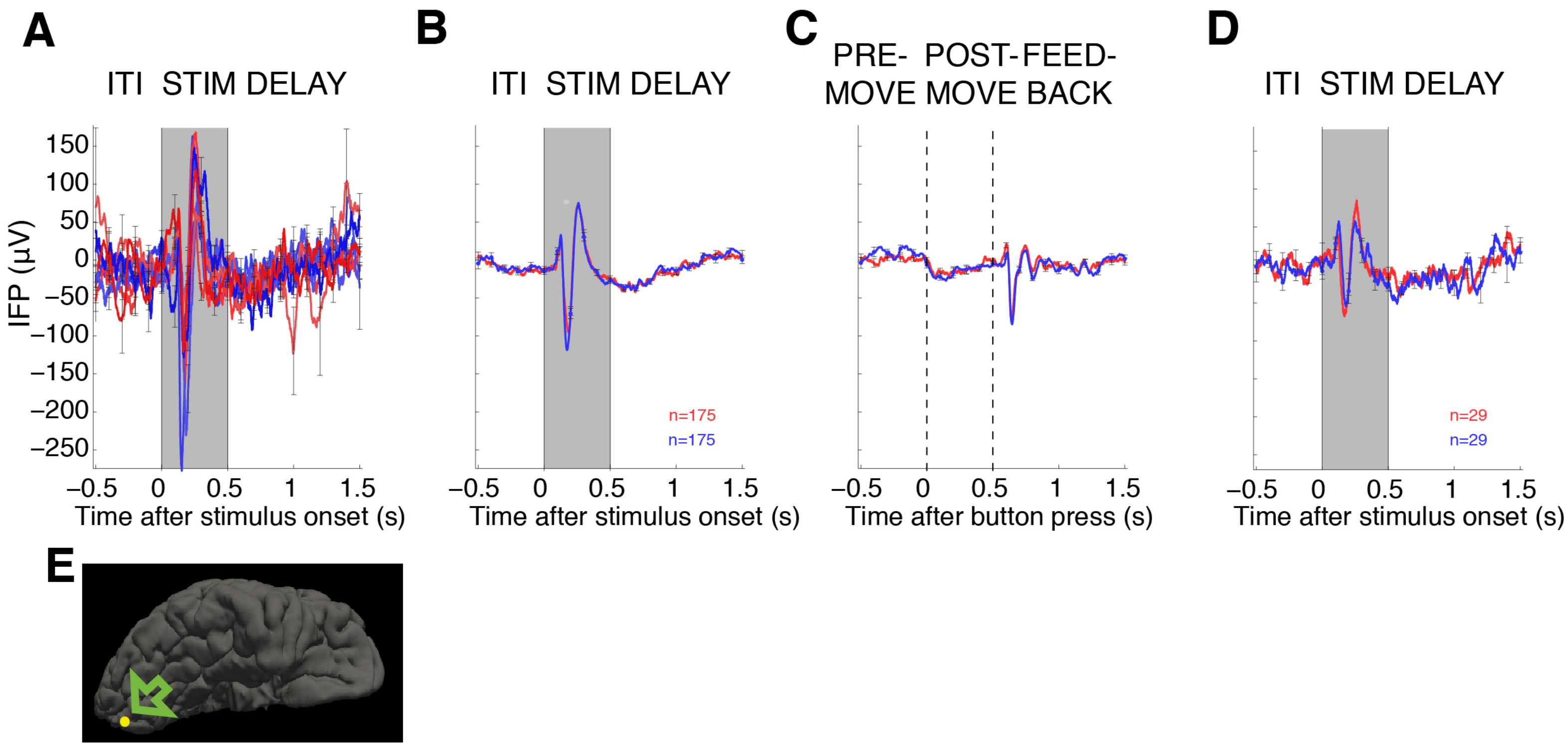

Figure S2: Example of a visually responsive electrode. Example responses during correct trials of a visually responsive electrode in the left inferior temporal gyrus (subject 7, electrode 52. Talairach coordinates = [-49.0, -46.6, -18.7]). Format is the same as **Figure 2B-E. A**. Responses to each stimulus shown separately (3 stimuli in each group). **B**. Average across stimuli within each group. **C**. Responses aligned to button press. **D**. Responses during error trials. **E**. Electrode location (arrow). This electrode showed a strong stimulus evoked response but did not differentiate between the two groups of stimuli.

Figure S3

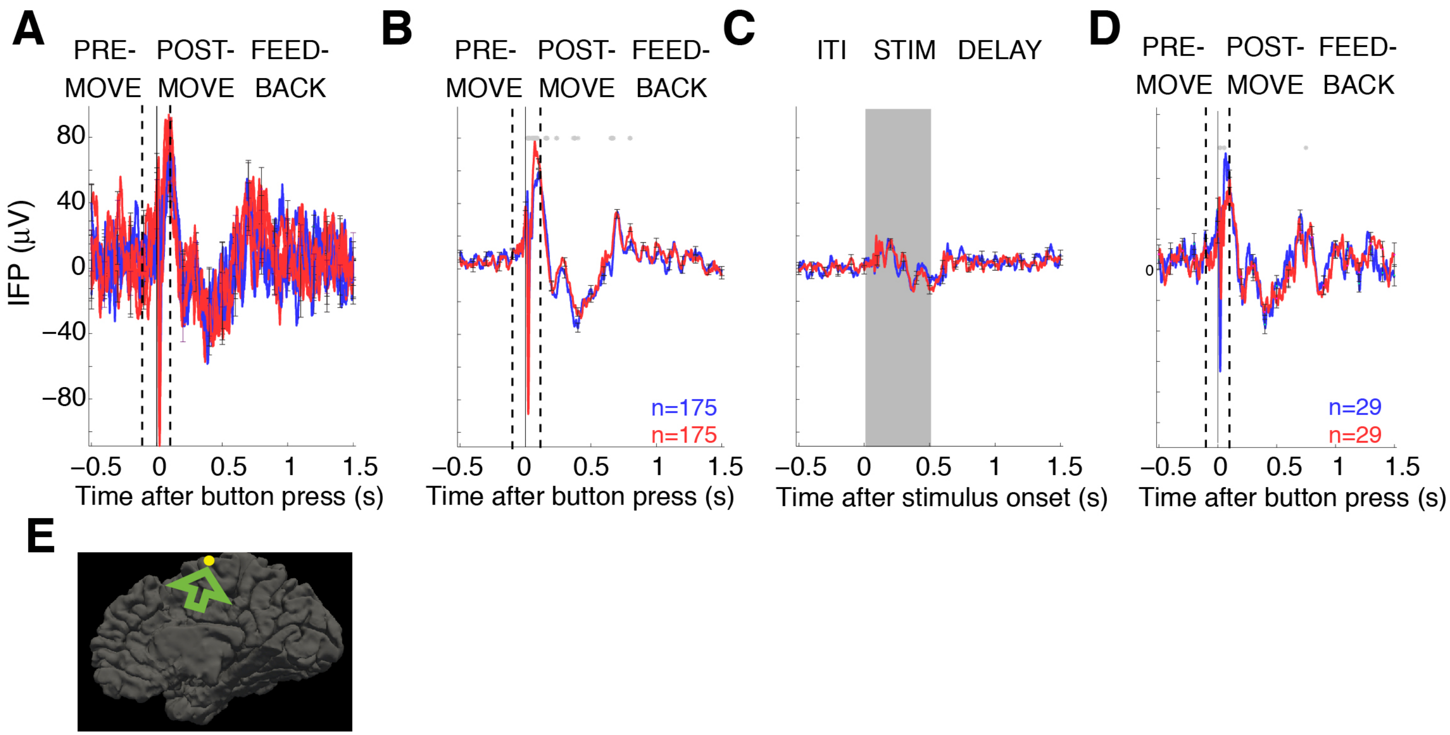

Figure S3: Example of a motor responsive electrode. Example responses during correct trials of a motor responsive electrode in the left postcentral gyrus (subject 7, electrode 123, Talairach coordinates = [49.4, -35.9, 58.6]). **A.** Responses to each stimulus shown separately, aligned to the button press (the colors correspond to the image borders in **Figure 2A**; the dashed lines denote the analysis interval, **Methods**). **B.** Responses averaged across stimuli within each group. **C** Responses aligned to the visual stimulus onset. **D**. Responses during error trials. **E.** Electrode location (arrow). This electrode showed a strong motor evoked response but did not differentiate between the two groups of stimuli.

Figure S4

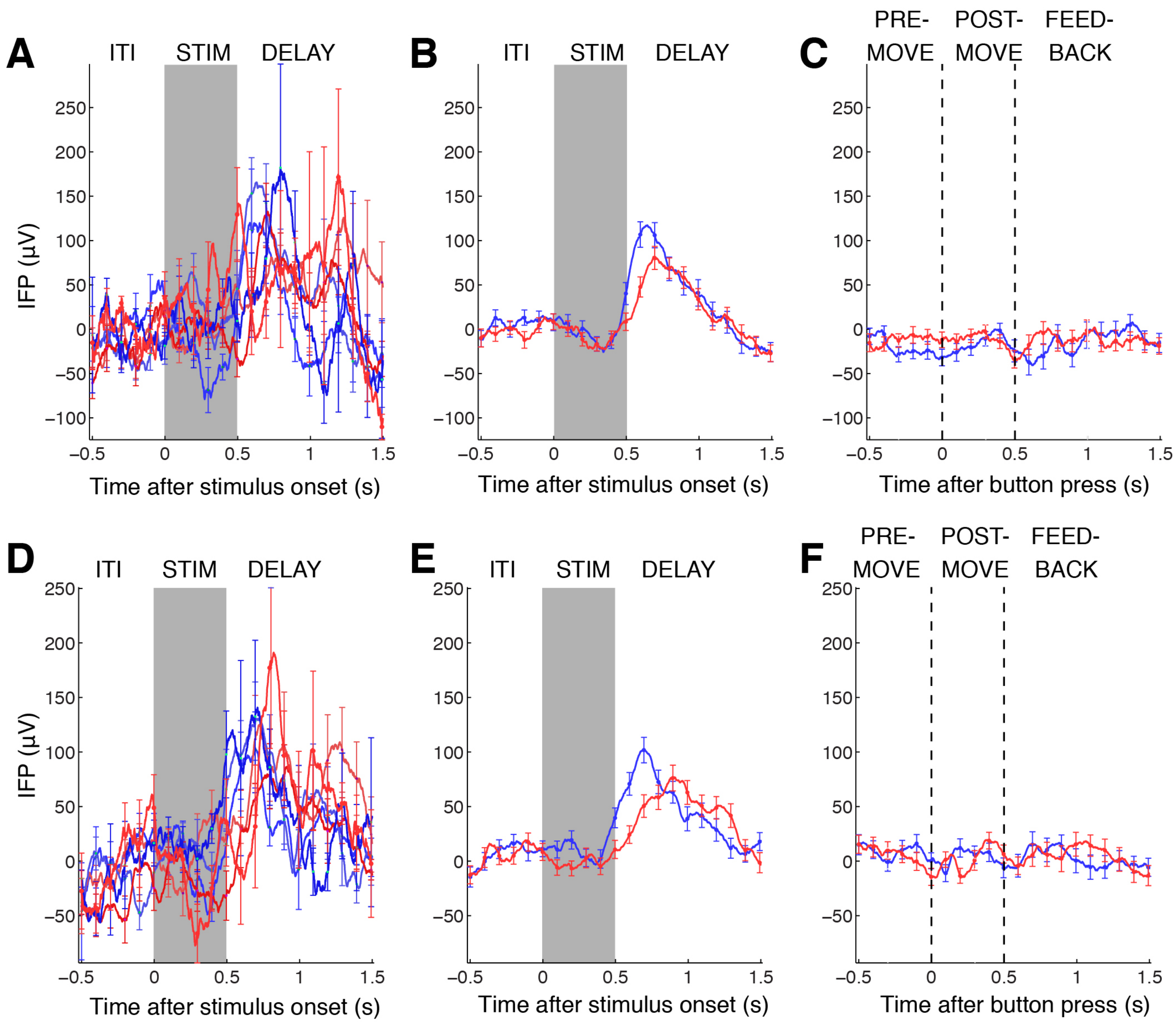

Figure S4: More examples of mapping selective electrodes. Expanding on **Figure 2** in the main text, this figure shows two additional examples of mapping selective electrodes from different subjects. The format follows the conventions in **Figure 2B-D**.

Figure S5

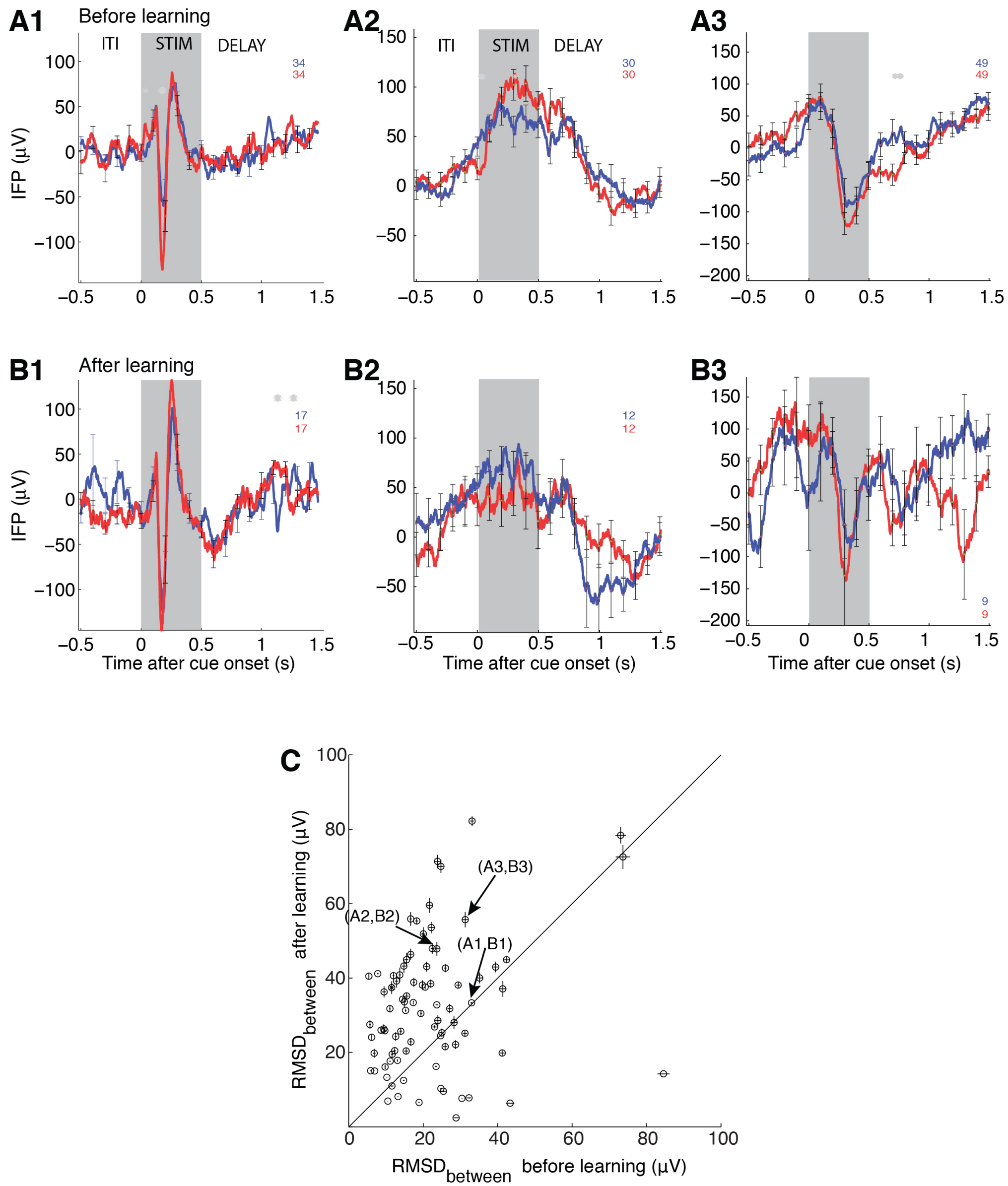

Figure S5: No effect of learning on visual responses. IFP responses from 3 example electrodes plotted separately before (**A**) and after (**B**) reaching learning criterion. The example in **A1**,**B1** is the same one shown in **Figure S1**. Format is similar to **Figure 3**. Here and in part **C**, the numbers of trials were balanced for comparisons across groups and learning conditions by random subsampling (shown on upper right). **C.** Root mean squared difference in IFP response between Group 1 and Group 2 stimuli, after (y-axis) vs. before (x-axis) learning for all visually responsive electrodes (n=87). The distribution of RMS differences in IFP amplitude between left and right mappings showed a weak effect of learning (*P*=0.03, permutation test). The arrows point to the example electrodes in parts **A-B**.

Figure S6

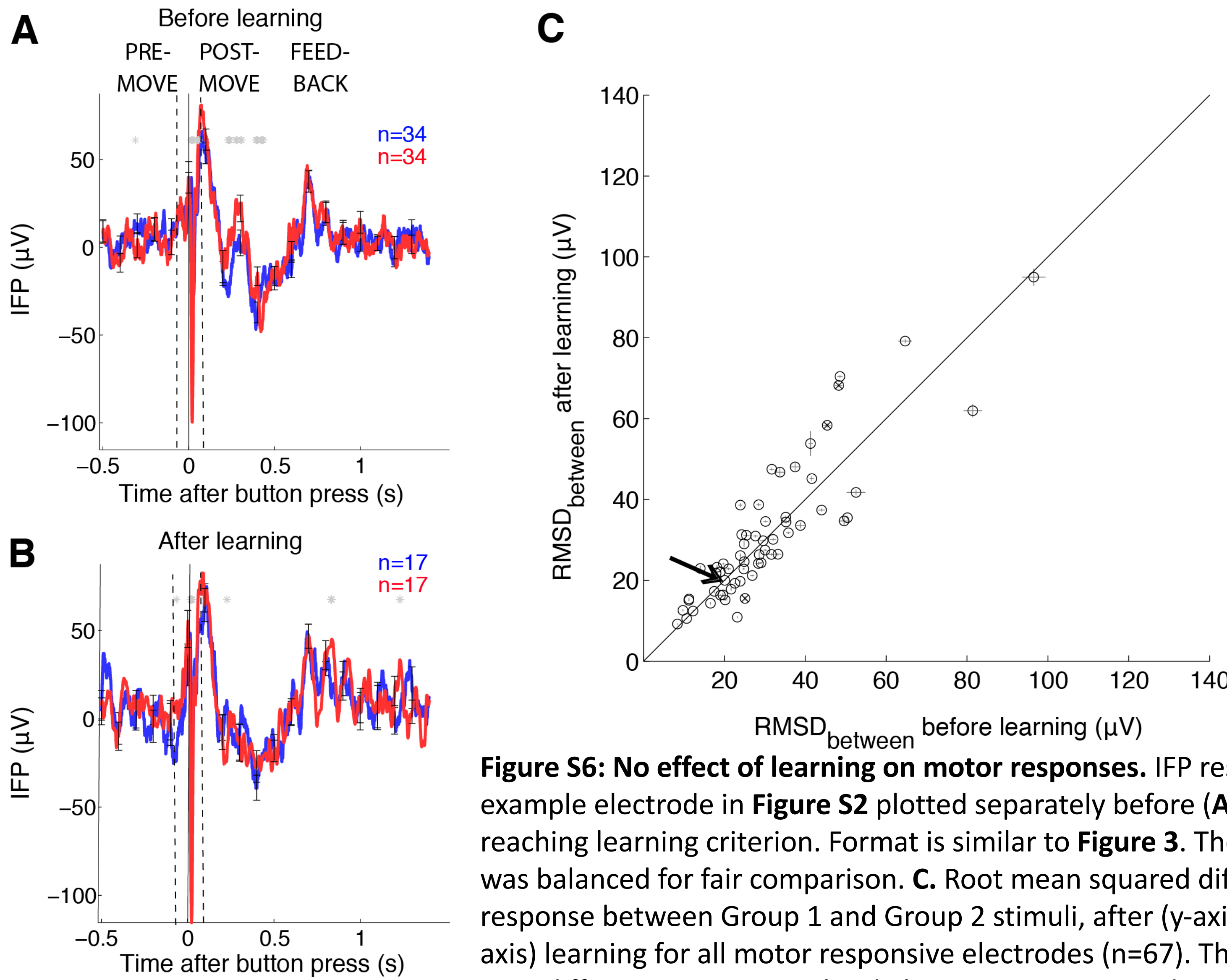

Figure S6: No effect of learning on motor responses. IFP responses from the example electrode in **Figure S2** plotted separately before (**A**) and after (**B**) reaching learning criterion. Format is similar to **Figure 3**. The number of trials was balanced for fair comparison. **C.** Root mean squared difference in IFP response between Group 1 and Group 2 stimuli, after (y-axis) vs. before (x-axis) learning for all motor responsive electrodes (n=67). The distribution of RMS differences in IFP amplitude between Group 1 and Group 2 stimuli showed no consistent trend with learning (*P*>0.01, two sided t-test). The arrow points to the example electrode in parts **A-B**.

Figure S7

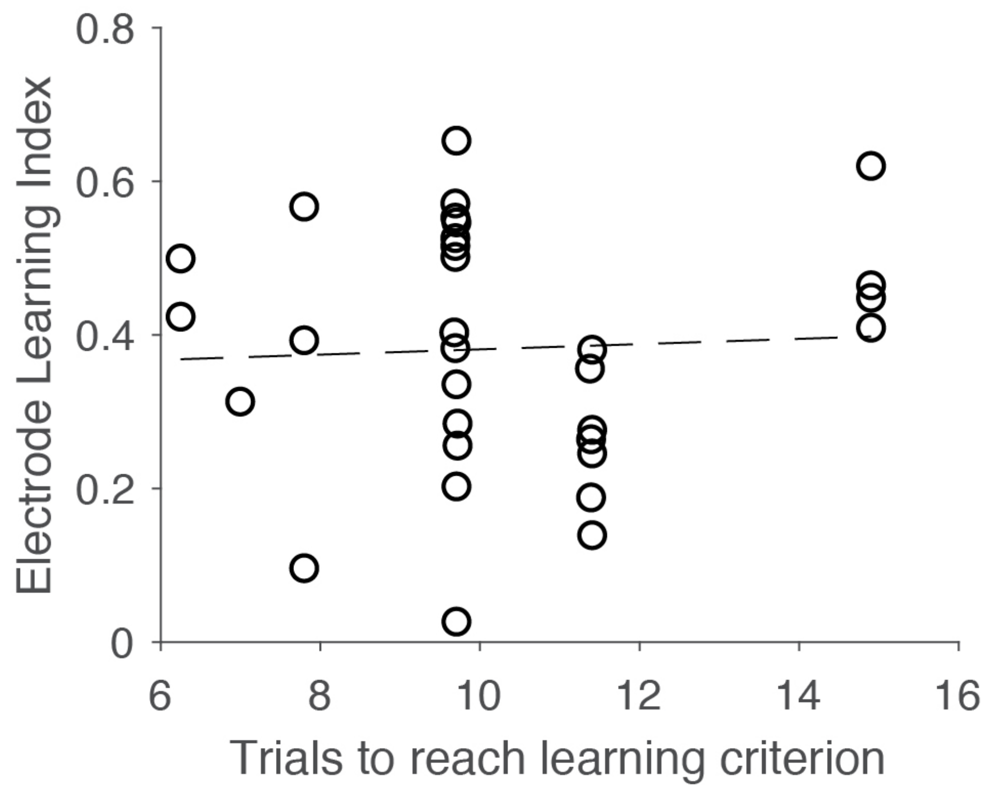

Figure S7: No correlation between task difficulty and physiological differences before and after learning. The y-axis shows the single electrode learning index defined by (RMSDbetween after learning – RMSDbetween before learning) / (RMSDbetween after learning + RMSDbetween before learning). The x-axis show the number of trials required to reach learning criterion (averaged across mappings for each electrode). The dashed line shows the linear fit. n=31 electrodes, as shown in **Figure 3**.

Figure S8

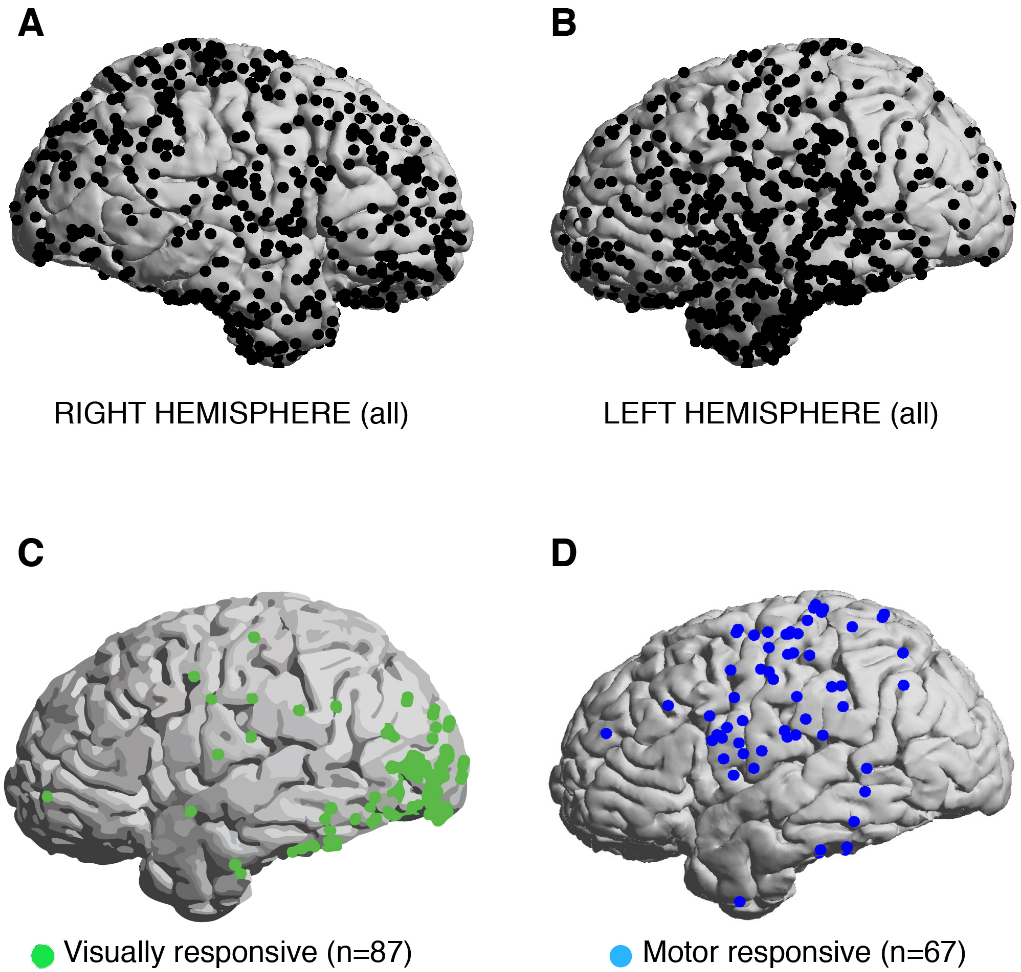

Figure S8: Electrode locations. (A-B) Location of all sampled electrodes (n=1240) (**C**) Location of visually responsive electrodes (n=87) and (**D**) motor selective electrodes (n=67). Here all electrodes were mapped onto one subject's brain (subject 5) for display purposes.

Figure S9

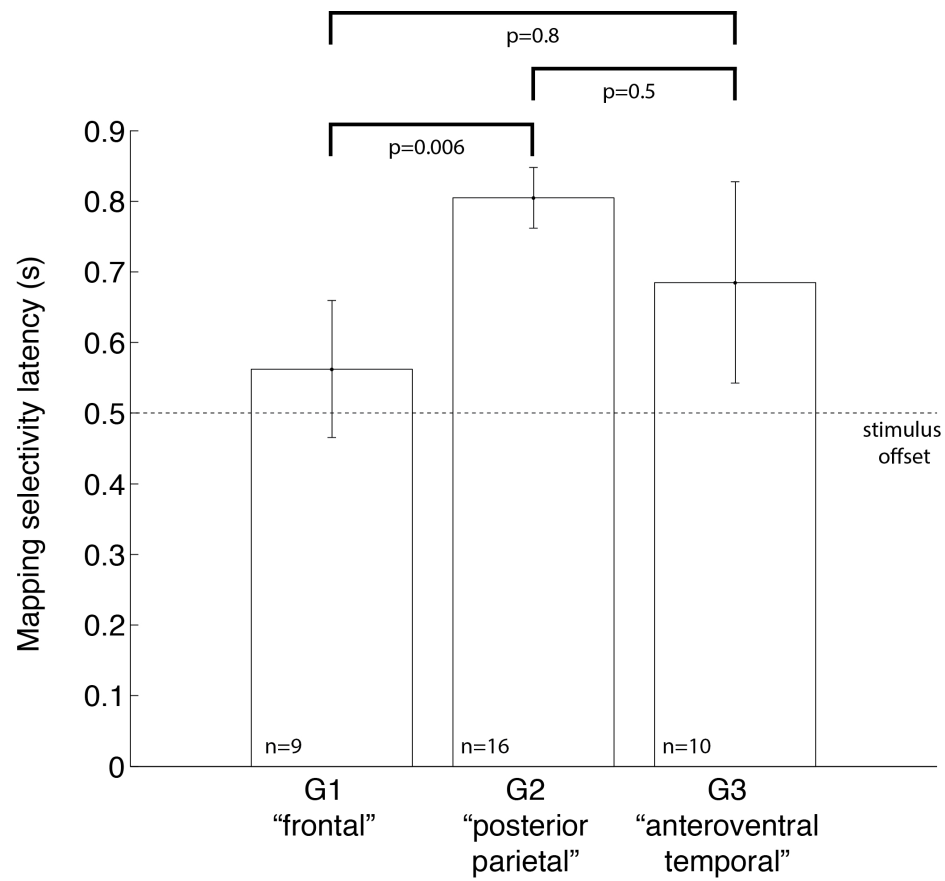

Figure S9: Earliest mapping selectivity in frontal cortex. Latency of mapping selective responses for the 3 anatomical groups of electrodes defined in **Figure 4**.

Figure S10A-F

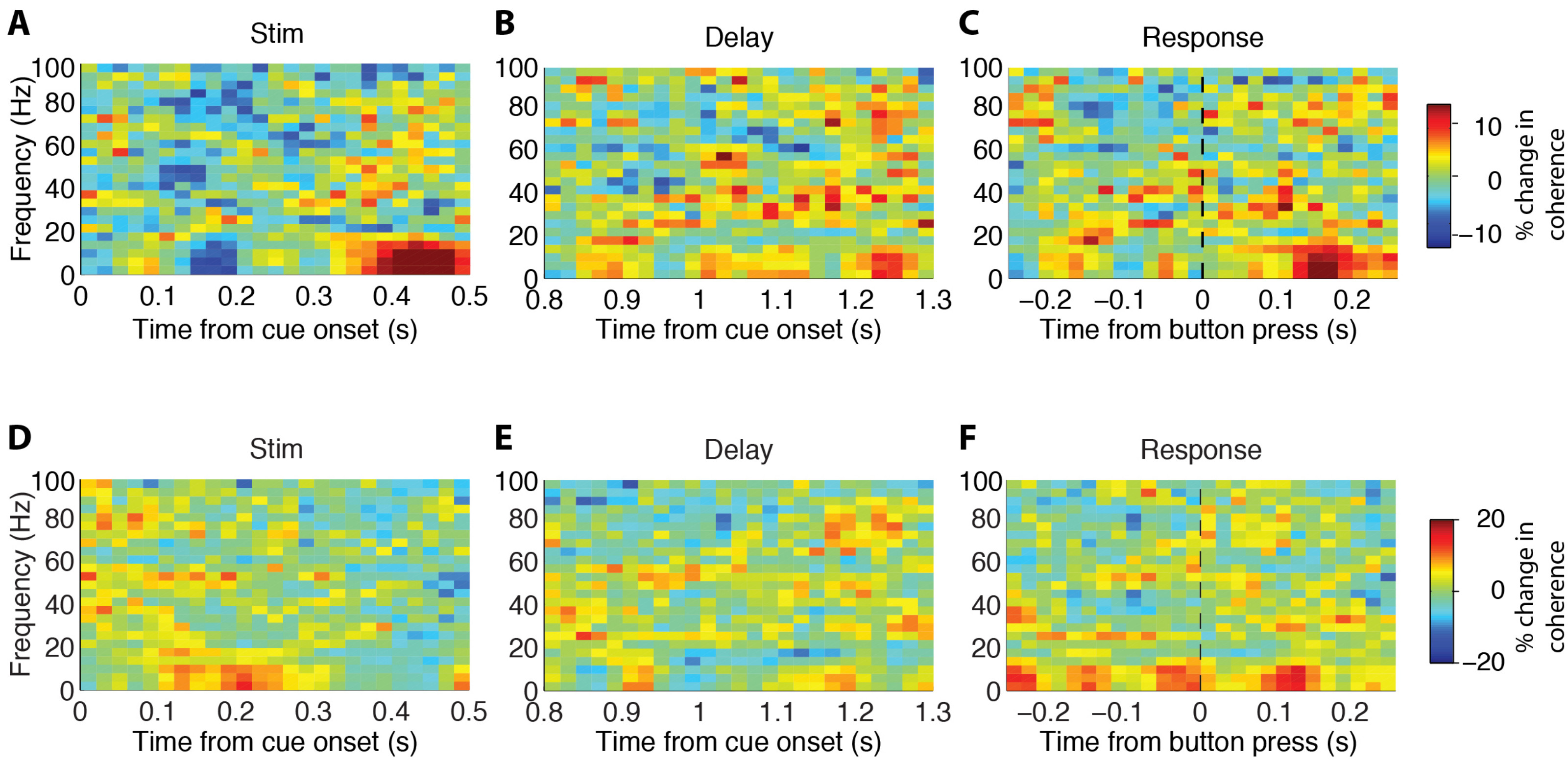

Figure S10A-F: More example coherograms. Expanding on **Figure 6** in the main text, this figure shows the coherogram between two pairs of electrodes (**A-C** and **D-F**). These electrode pairs come from Subject 11, a different subject from the one shown in **Fig. 6**. The format and conventions follow those in **Fig. 6A-C**. In both cases, one electrode is visually responsive and the other one is a mapping selective electrode. The number of trials was n=203. These examples appear qualitatively different from those in **Fig. 6A-C** and are presented here to illustrate the heterogeneity of the coherence change dynamics. In both electrode pairs there was a larger change in coherence during the delay period compared to baseline.

Figure S10G-H

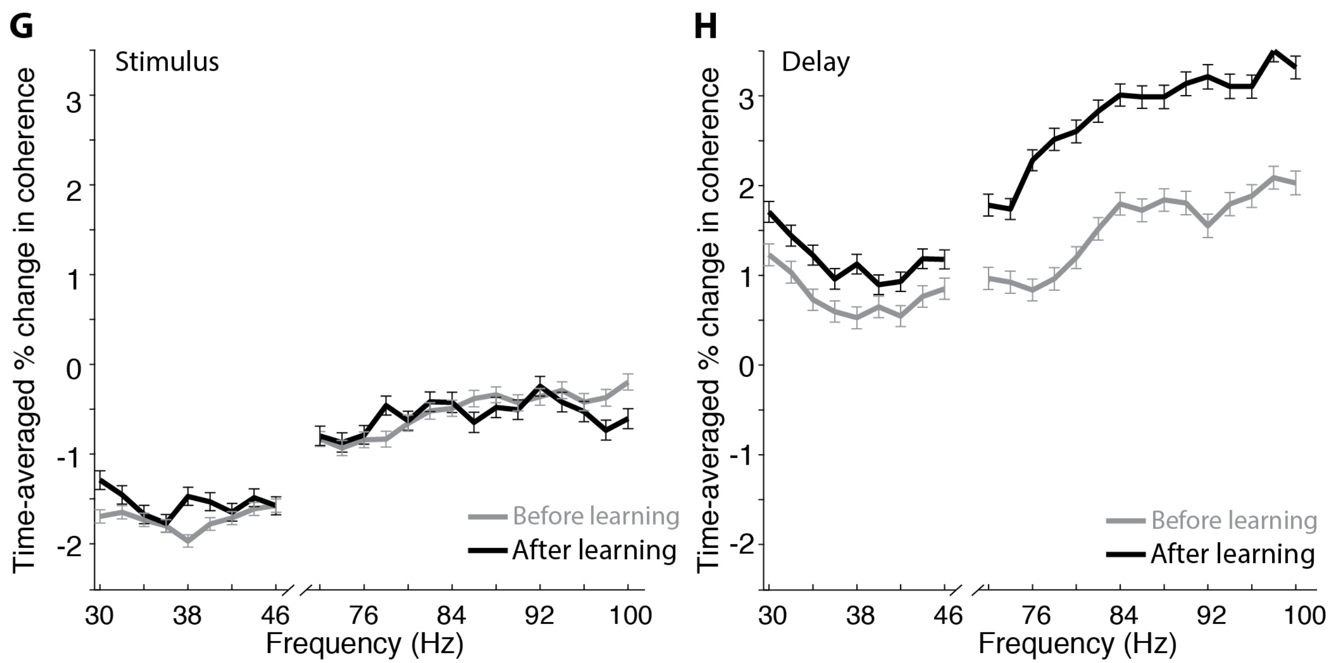

Figure S10G-H: Time-averaged coherograms. Expanding on **Figures 6-7** in the main text, this figure shows the coherogram averaged over time during the stimulus period (**G**) or delay period (**H**) as a function of frequency for those trials before learning (gray) and those trials after learning (black). The interval centered around 60 Hz was not considered for the analyses.

Figure S11

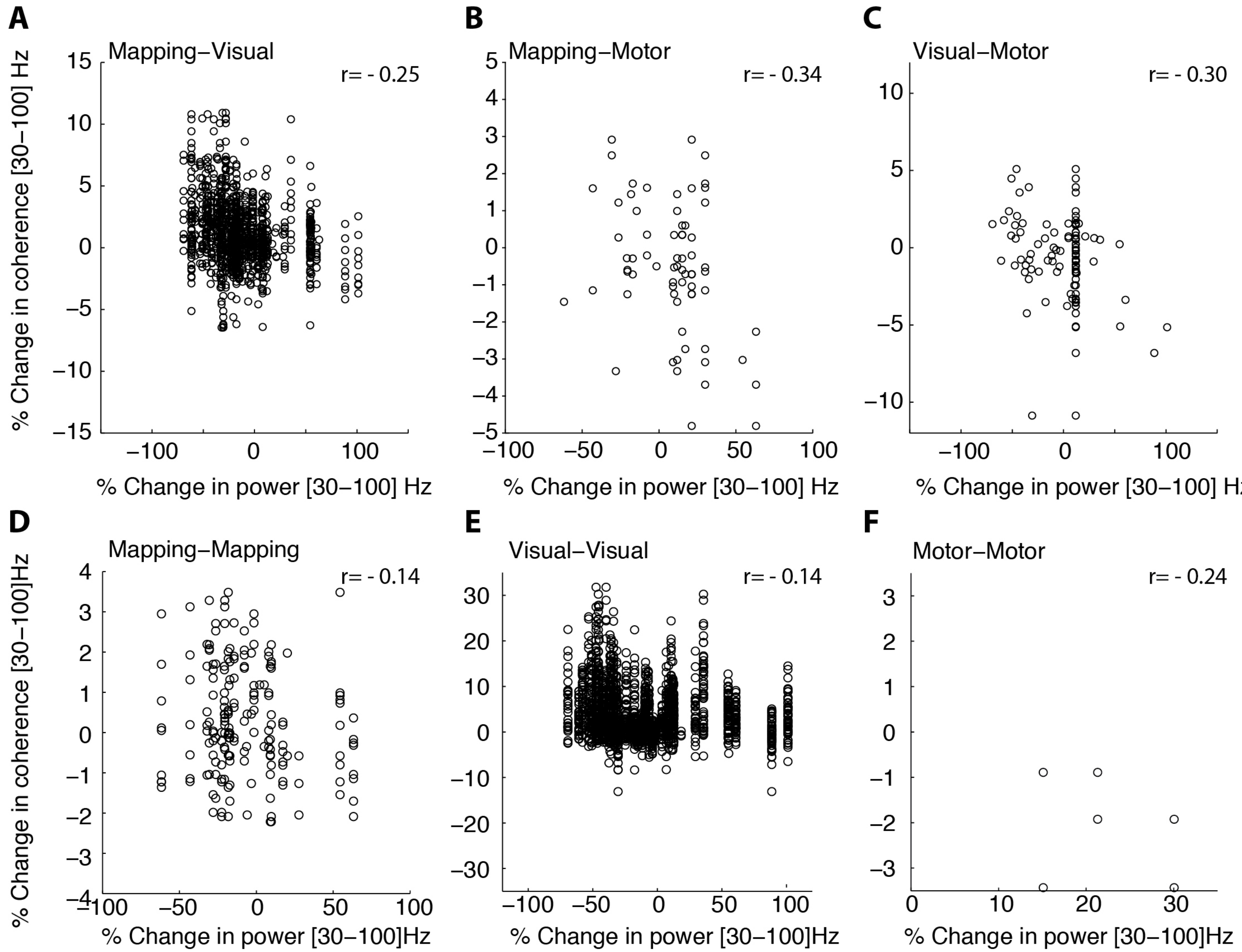

Figure S11: Increase in coherence was not accompanied by increase in single electrode power. Expanding on **Figure 6** in the main text, this figure shows the change in gamma band coherence with respect to baseline during the delay period (y-axis) as a function of the change in power in the gamma band during the delay period, averaged over the two electrodes for each electrode pair. Each point corresponds to one electrode pair. Each subplot shows a different subset of electrode pairs (corresponding to the 6 different groups in **Figures 6G-H**.

Figure S12

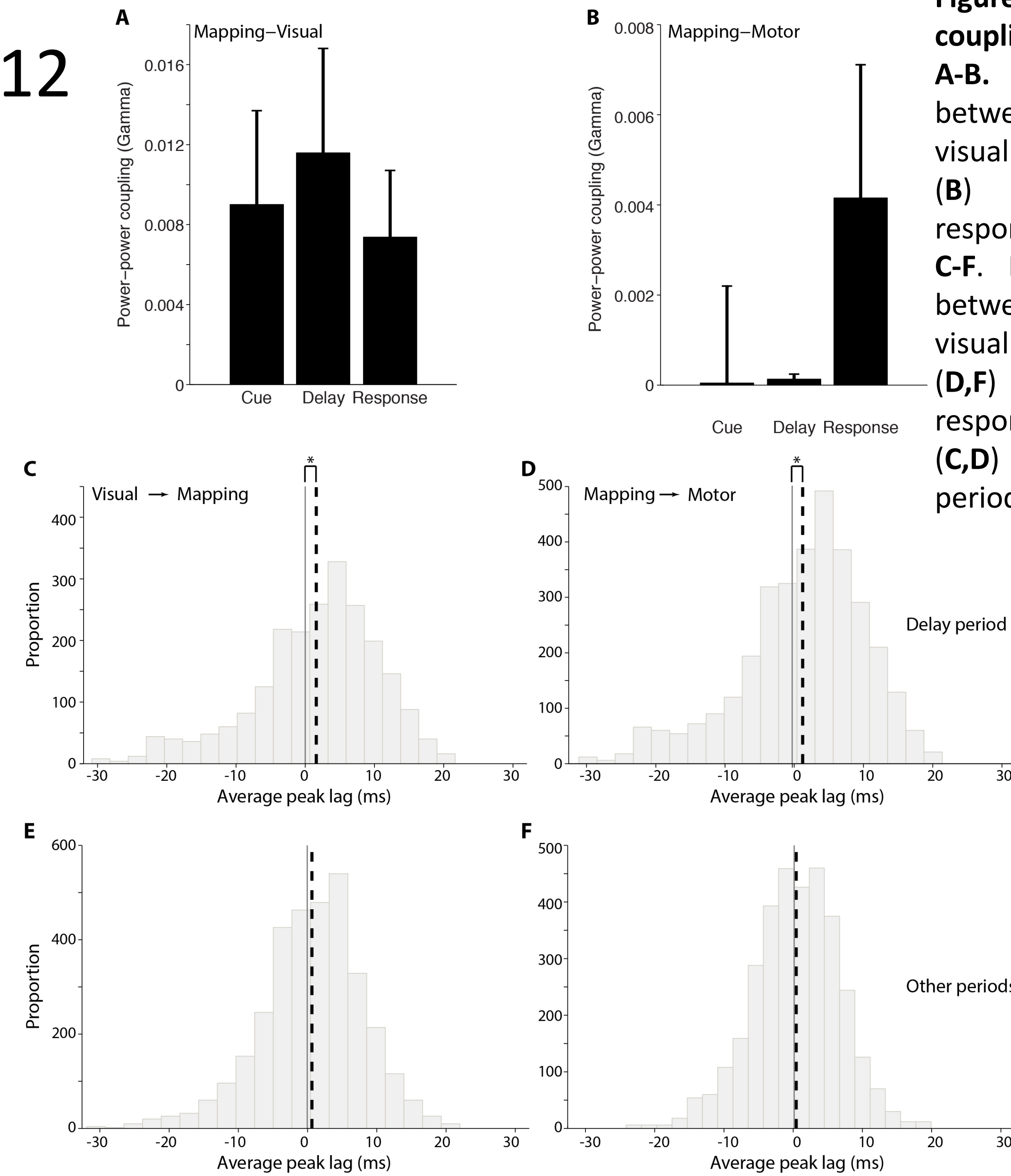

Figure S12: Power-power coupling in the gamma band.

A-B. Power-power coupling between (**A**) mapping and visually responsive electrodes; (**B**) mapping and motor responsive electrodes.

C-F. Distribution of peak lags between (**C,E**) mapping and visually responsive electrodes; (**D,F**) mapping and motor responsive electrodes during the (**C,D**) delay period; (**E,F**) other periods.